BIOCHEMISTRY
including biophysical chemistry & molecular biology

Article

pubs.acs.org/biochemistry

Flight of a Cytidine Deaminase Complex with an Imperfect Transition State Analogue Inhibitor: Mass Spectrometric Evidence for the Presence of a Trapped Water Molecule

Gottfried K. Schroeder,*[,†,§] Li Zhou,[†] Mark J. Snider,[‡] Xian Chen,[†] and Richard Wolfenden*[,†]

[†]Department of Biochemistry and Biophysics, University of North Carolina, Chapel Hill, North Carolina 27599, United States
[‡]Department of Chemistry, College of Wooster, Wooster, Ohio 44691, United States

Supporting Information

ABSTRACT: Cytidine deaminase (CDA) binds the inhibitor zebularine as its 3,4-hydrate ($K_d \sim 10^{-12}$ M), capturing all but ~5.6 kcal/mol of the free energy of binding expected of an ideal transition state analogue ($K_{tx} \sim 10^{-16}$ M). On the basis of its entropic origin, that shortfall was tentatively ascribed to the trapping of a water molecule in the enzyme−inhibitor complex, as had been observed earlier for product uridine [Snider, M. J., and Wolfenden, R. (2001) *Biochemistry 40*, 11364−11371]. Fourier transform ion cyclotron resonance mass spectrometry (FTICR-MS) of CDA nebularized in the presence of saturating 5-fluorozebularine reveals peaks corresponding to the masses of $E_2Zn_2W_2$ (dimeric Zn-CDA with two water molecules), $E_2Zn_2W_2Fz$, and $E_2Zn_2W_2Fz_2$, where Fz represents the 3,4-hydrate of 5-fluorozebularine. In the absence of an inhibitor, E_2Zn_2 is the only dimeric species detected, with no additional water molecules. Experiments conducted in $H_2{}^{18}O$ indicate that the added mass W represents a trapped water molecule rather than an isobaric ammonium ion. This appears to represent the first identification of an enzyme-bound water molecule at a subunit interface (active site) using FTICR-MS. The presence of a 5-fluoro group appears to retard the decomposition of the inhibitory complex kinetically in the vapor phase, as no additional dimeric complexes (other than E_2Zn_2) are observed when zebularine is used in place of 5-fluorozebularine. Substrate competition assays show that in solution zebularine is released from CDA ($k_{off} > 0.14$ s^{-1}) much more rapidly than is 5-fluorozebularine ($k_{off} = 0.014$ s^{-1}), despite the greater thermodynamic stability of the zebularine complex.

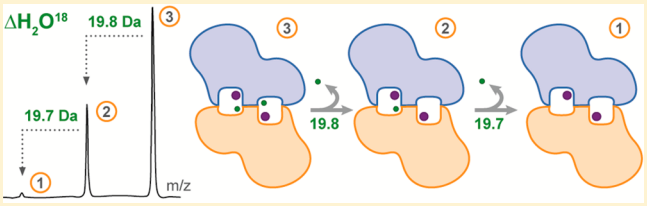

The minimal affinity of an enzyme for the altered substrate in the transition state ($S^{‡}$) can be estimated by comparing the enzyme-catalyzed and uncatalyzed reaction rates and establishes a benchmark against which the effectiveness of potential transition state analogue inhibitors can be tested.[1−3] That information has been reported[4] for the complex formed between the potent transition state analogue inhibitor 3,4-dihydrouridine [DHU (Figure 1)] and *Escherichia coli* cytidine deaminase (CDA, EC 3.5.4.5), a dimeric zinc enzyme that catalyzes the conversion of cytidine to uridine and is structurally and mechanistically related to the ApoB RNA-editing family of enzymes.[5] In CDA, two symmetrically situated active sites are present at the dimer interface, each containing the split elements of a substrate water molecule, with a hydroxide ion bound by the zinc atom and a proton bound by the carboxylate group of Glu-104.[6]

As illustrated in Figure 1, the structure of the CDA−DHU complex suggests that during deamination, the 3,4-double bond of cytidine becomes covalently hydrated with addition of H^+ at N3 and addition of OH^- at C4, forming a tetrahedral intermediate that approaches the transition state in structure.[7] Ammonia is then eliminated, with rate-determining C−N bond cleavage,[6] to yield the product uridine.

Crystal structures of inhibitory complexes of CDA with zebularine (Zeb),[7] or with the related inhibitor 5-fluorozebularine (FZeb),[8] show that both these inhibitors are bound as covalently hydrated species (Figure 1B) that resemble a tetrahedral intermediate approaching the presumed transition state for the deamination of cytidine, with cytidine covalently hydrated at the 3,4-double bond (Figure 1A). Figure 1B shows that in these enzyme−inhibitor complexes the elements of substrate water that were originally split between the zinc atom and Glu-104 are incorporated into DHU.

Effects of temperature on the K_d value of DHU, and the direct calorimetric titration of CDA with Zeb, indicate that the binding of DHU is associated with a large and favorable change in enthalpy ($\Delta H = -21.1$ kcal/mol), closely matching the estimated enthalpy change associated with the binding of $S^{‡}$ itself ($\Delta H = -20.2$ kcal/mol). In contrast to the binding of $S^{‡}$ ($T\Delta S = 1.6$ kcal/mol), the binding of DHU is achieved at an entropic cost ($T\Delta S$) of −4.9 kcal/mol. That entropic penalty (−5 kcal/mol) is also observed in the formation of the enzyme−product complex with uridine, in which a trapped water molecule is observed crystallographically (green sphere in Figure 1).[9] The crystal structure of the enzyme−inhibitor

Received: April 20, 2012
Revised: July 6, 2012
Published: July 9, 2012

dx.doi.org/10.1021/bi300516u | *Biochemistry* 2012, 51, 6476−6486

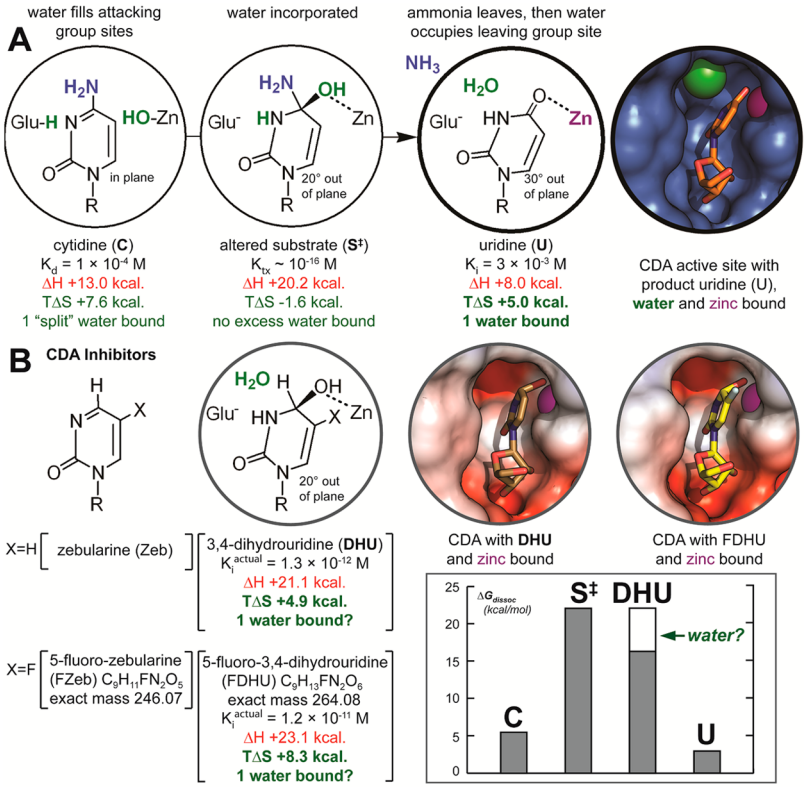

Figure 1. Thermodynamic changes associated with binding of ligands on the reaction pathway (A) and inhibitors (B).[4] Equilibrium constants and thermodynamic parameters are shown for dissociation. Thermodynamic parameters for FDHU release were determined in this work. Crystal structure figures were generated using PyMOL.[10] The active site electrostatic surface potentials (in panel B) were generated with the Adaptive Poisson–Boltzmann Solver (APBS)[11] using the AMBER force field (PyMOL APBS Tools 2.1 plugin, M. G. Lerner) and the conversion program PDB2PQR.[12,13] Red indicates negative charge, blue positive charge, and white hydrophobic areas.

Scheme 1. Proposed Sequence of Events within the Mass Spectrometer following Nebularization of the Complex of the Dimeric Enzyme (blue and orange) with FDHU (yellow), Zinc (purple), and a Trapped Water Molecule (green) at the Active Site(s)[a]

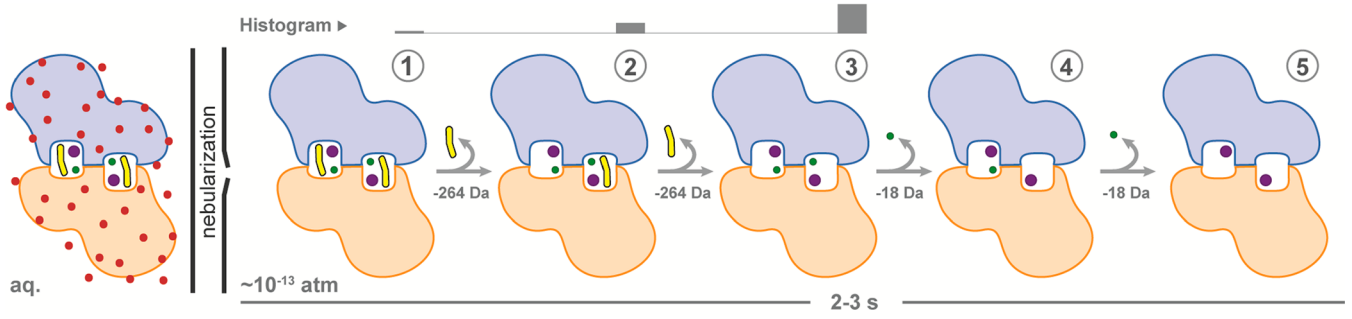

[a]The vacuum within the analysis chamber (~10^{-13} atm) is sufficient to remove all solvating water molecules (red), yielding the dimer (1). Presumably, the bound molecules "leak" out during the analysis time (2–3 s), yielding the various species shown (1–5), corresponding to the indicated losses in mass. The dimeric species (3) corresponds to the most prevalent resultant mass peak observed previously, as indicated by the top panel histogram (data taken from ref 14).

complex[7] indicates the presence of a gap in the polar leaving group site (Figure 1B, electrostatic surface potential images)[10–13] expected to be occupied by the ammonia leaving group during deamination. It was suggested that the trapping of an "extra" water molecule in the enzyme–inhibitor complex might account for the entropic penalty observed and for the enzyme's less-than-perfect binding of DHU (Figure 1, chart).

In earlier work,[14] we sought to test the possibility that a water molecule in the enzyme–inhibitor complex might be detectable using Fourier transform ion cyclotron resonance mass spectrometry (FTICR-MS). Scheme 1 outlines a plausible sequence of events in the mass spectrometer, beginning with the nebularization of the dimeric enzyme complex with FDHU from aqueous solution. Under nondenaturing conditions in the absence of an inhibitor, the most significant mass corresponded to that of the dimeric enzyme with two zinc atoms and no water molecules (Scheme 1, stage 5). Evidently, all unbound water molecules were stripped from the protein during nebularization. In the presence of the fluorinated inhibitor FZeb, three dimeric protein masses were evident (Scheme 1, stages 1–3). The most significant of these corresponded to the mass of the dimeric enzyme with two zinc atoms and two water

dx.doi.org/10.1021/bi300516u | Biochemistry 2012, 51, 6476–6486

molecules (Scheme 1, stage 3). The less prominent second and third peaks were augmented by the mass of covalently hydrated FZeb (FDHU). The histogram in the top panel of Scheme 1 indicates the relative magnitudes of these peaks. Because those preliminary experiments were conducted in the presence of low concentrations of ammonium acetate buffer, the origin of the additional mass of ~35 Da attributed to two water molecules (Scheme 1, stage 3) could not be identified unambiguously. Earlier kinetic experiments had shown that *E. coli* CDA displays a weak affinity for NH_4^+ as an inhibitor.[15] However, the molecular mass of NH_4^+ is essentially indistinguishable from that of water (18 Da), leaving open the possibility that an ammonium ion rather than a water molecule might be responsible for the observed increment in mass. Interestingly, preliminary attempts to repeat this experiment in the presence of Zeb failed to show any noncovalent association of the enzyme with either water or an inhibitor (Scheme 1, stage 5). The experiments were undertaken to address the identity of the trapped molecule in the dimeric enzyme−inhibitor complexes and the surprising failure of Zeb to stabilize such complexes in the vapor phase.

In this work, CDA was found to be mainly monomeric in the vapor phase in the absence of inhibitor, as described previously.[14] In the presence of the powerful inhibitor FZeb, we observed masses corresponding to the dimeric enzyme−inhibitor complexes described previously, including those containing the added masses of two molecules of $H_2{}^{16}O$ (36 Da) or NH_4^+ (36 Da) (Scheme 1, stages 1−4). To determine whether those increments in mass were due to water or the ammonium ion, we conducted the same experiment in the presence of $H_2{}^{18}O$. If one or two molecules of $H_2{}^{18}O$ were bound at the active site, as opposed to NH_4^+, then an additional shift of 2 or 4 Da (distinguishable in principle with the ultrahigh mass accuracy of <1 ppm provided by an instrument with a 12 T magnet) would be expected (Scheme 1, stages 3−5). In all experiments with FZeb, the peak with two bound water molecules (Scheme 1, stage 3) consistently exhibited the highest signal-to-noise ratio. To look for the potential incorporation of $H_2{}^{18}O$, it therefore seemed reasonable to focus our analysis on that peak.

In preliminary experiments, dimeric enzyme complexes with the added mass of water (or NH_4^+) were not observed in the presence of Zeb. This observation is surprising in view of the fact that that DHU is bound ~10-fold more tightly[4] than FDHU[16] (for K_i^{actual} values, see Figure 1B). Earlier work[17] showed that DHU is formed rapidly and reversibly from Zeb at the enzyme's active site. Surprisingly, preliminary experiments suggested that the same might not be true of FZeb, and that a slightly larger 5-fluorine substituent might have a substantial retarding effect on the binding and release of FDHU, in addition to its effect on the thermodynamics of binding. Such an effect, if present, would be expected to be manifest in either the vapor phase or the liquid phase.

To determine whether the rates of association of FZeb with and dissociation of FZeb from the enzyme are slow in solution, we used stopped-flow fluorescence and competition assays. The relative contributions of enthalpy and entropy to FDHU−CDA complex dissociation were estimated by isothermal titration calorimetry (ITC) experiments using FZeb, and van't Hoff analysis of the temperature dependence of the equilibrium constant for FZeb hydration using model compounds. To complete the thermodynamic analysis, it was also necessary to establish the affinity of the enzyme for 5-fluorocytidine in the transition state for its deamination. Accordingly, we measured its rate of nonenzymatic hydrolysis and the values of k_{cat} and K_M for the enzyme-catalyzed reaction. The effects of a single hydrogen-to-fluorine substitution on the kinetic and thermodynamic characteristics of inhibitor binding (Zeb vs Feb) were also investigated.

MATERIALS AND METHODS

High-performance liquid chromatography grade water and glacial acetic acid were purchased from Fisher Scientific (Pittsburgh, PA). $H_2{}^{18}O$ (97 ^{18}O at. %) was obtained from ISOTEC-Sigma (St. Louis, MO). Zeb and FZeb were gifts from V. Marquez (National Cancer Institute, National Institutes of Health, Bathesda, MD). Cation exchange resin (50W-X8, 100−200 mesh, hydrogen form) was obtained from Bio-Rad (Hercules, CA). Other chemicals were obtained from TCI America (Portland, OR) or Sigma-Aldrich Co. Recombinant CDA from *E. coli* was overexpressed in *E. coli* and purified as previously reported.[18,19]

FTICR-MS Analysis. Enzyme samples (3×10^{-5} M in monomer) were dialyzed overnight into ammonium acetate buffer (5×10^{-3} M) at pH 5.6, where CDA maintains essentially full activity.[16] For experiments conducted under nondenaturing conditions, enzyme samples were then mixed with (A) $H_2{}^{16}O$, (B) FZeb (2.3×10^{-4} M) in $H_2{}^{16}O$, or (C) FZeb (2.3×10^{-4} M) in $H_2{}^{18}O$. Immediately before MS analysis, all samples were acidified slightly with glacial acetic acid (final concentration of 0.5% by volume), without the addition of other organic solvents, to assist nebulization. For experiments conducted under denaturing conditions, enzyme samples were prepared in a 50% methanol and 2% acetic acid solution immediately before nebularization.

MS spectra were acquired using a hybrid Qe-Fourier transform ion cyclotron resonance mass spectrometer, equipped with a 12.0 T actively shielded magnet (Apex Qe-FTICR-MS, 12.0 T AS, Bruker Daltonics, Billerica, MA), and an Apollo II microelectrospray ionization (μESI) source. The voltages on the μESI sprayer, interface plate, heated capillary exit, deflector, ion funnel, and skimmer were set at 4.3 kV, 3.9 kV, 300 V, 250 V, 175 V, and 80 V, respectively. The temperature of the μESI source was maintained at 180 °C. Desolvation was conducted using both nebulization gas flow (2.0 bar) and countercurrent drying gas flow (4.0 L/s). All samples were directly infused using a syringe pump (Harvard Apparatus, Holliston, MA) equipped with a 250 μL syringe (Hamilton, Reno, NV), at an infusion flow rate of 90 μL/h. Before transfer, ion packets accumulated inside the collision cell for a fixed duration of 1−3 s. For each spectrum, 100 MS scans were acquired in the ICR cell with a resolution of 580000 at an m/z of 400 Da.

Pre-Steady State Kinetics for the Release of FZeb or Zeb. The off rate constant (k_{off}) for the transition state analogue inhibitor FZeb (or Zeb) was determined as follows. CDA was preincubated with FZeb (or Zeb) at a concentration in 10-fold excess of the $K_i^{observed}$ value. After a preincubation period of 5, 20, or 35 min, inhibited CDA was diluted 100-fold into a concentrated solution of substrate cytidine (10-fold excess of K_M). The conversion of cytidine to uridine was then monitored by the change in UV absorbance at 282 nm ($\Delta\varepsilon$ = −3600 M^{-1} cm^{-1}) on a Hewlett-Packard diode array 8452a spectrophotometer for 10 min. The steady state rate was extrapolated from the final 200 s of the reaction (linear portion). A "lag" in the approach to the extrapolated steady

dx.doi.org/10.1021/bi300516u | *Biochemistry* 2012, 51, 6476−6486

state turnover rate was used to determine the off rate constant for the inhibitor.

Pre-Steady State Kinetics for the Binding of FZeb. The intrinsic fluorescence of the inhibitor FZeb is quenched upon binding to CDA.[16] A rapid mixing device (RX.1000, Applied Photophysics Ltd., Leatherhead, U.K.) and a spectrofluorometer (Fluorolog-3, Horiba Jobin Yvon Inc., Edison, NJ) were used to monitor the decay in FZeb fluorescence as a function of time with increasing enzyme concentration. Bandpass filter widths were set at 2 mm, and the fluorescence excitation and emission wavelengths were 322 and 390 nm,[16] respectively. In a typical experiment (25 °C), one reservoir of the rapid mixing device was filled with a solution containing FZeb (0.1 μM, after mixing), while the second contained a CDA solution of varying concentrations (from ~0.1 to ~0.8 μM, after mixing). Fluorescence acquisition was initiated when the two solutions were mixed at a 1:1 ratio, with a total dead time of ~0.4 s. The fluorescence data were interpreted according to the kinetic scheme shown in eq 1

$$\mathrm{E} + \mathrm{I} \underset{k_{off}}{\overset{k_{on}}{\rightleftarrows}} \mathrm{EI} \tag{1}$$

where E is the enzyme, I the inhibitor, and EI the enzyme−inhibitor complex. All kinetic traces represent an average of a minimum of five experimental runs (2 min each) and were fit by nonlinear regression to eq 2

$$[\mathrm{I}] = Ae^{-k_{obs}t} + B \tag{2}$$

where t is the time, $k_{obs} = k_{observed}$, and A and B are constants. The resultant apparent first-order rate constants (k_{obs}) showed a linear relationship to enzyme concentration (eq 3)

$$k_{obs} = k_{on}[\mathrm{E}] + k_{off} \tag{3}$$

and an initial estimate for the on rate constant (k_{on}) was determined from a plot of k_{obs} versus enzyme concentration. This value and the value for k_{off} determined above were used as starting parameters for fitting by simulation (KinTek Explorer, KinTek Corp., Austin, TX),[20] using the model shown in eq 1.

Steady State Kinetics of Deamination. Enzyme assays (2.5 nM in dimer) were conducted in potassium phosphate buffer (0.1 M, pH 6.8) at 25 °C, following initial rates. Cytidine (ε_{290} = 2200 M^{-1} cm^{-1}) deamination was monitored at 290 nm ($\Delta\varepsilon$ = −1750 M^{-1} cm^{-1}), and 5-fluorocytidine deamination was monitored at 292 nm ($\Delta\varepsilon$ = −3500 M^{-1} cm^{-1}). Extinction coefficients of 5-fluorocytidine (ε_{292} = 5950 M^{-1} cm^{-1}) and 5-fluorouridine (ε_{292} = 2450 M^{-1} cm^{-1}) were experimentally determined on the basis of the reported spectral properties of these compounds.[21]

Synthesis of 1-*N*-Methyl-5-fluorocytosine. The synthetic procedure was adapted from a procedure described previously[22] for the methylation of cytosine. 5-Fluorocytosine (0.32 mmol) was dissolved in water (3 mL) containing NaOH (0.16 M) and allowed to react with trimethylphosphate (0.9 mL, 25 equiv) for 24 h at room temperature. Basic reaction conditions (pH 13) were maintained during the course of the reaction by addition of NaOH (5 M). Residual trimethylphosphate was removed by evaporation (Kugelrohr), and the major product of the reaction (~95%) was the dimethylphosphate salt of the desired compound. The product was desalted using an anion exchange resin (100−200 mesh AG 1-X8, Bio-Rad, Hercules, CA) and recrystallized from a minimal amount of water at 4 °C, yielding fine crystals of the title compound: λ_{max} = 282 nm (pH 7, water), δ_H (D_2O 500 MHz) 7.70 (1H, d, J = 5.8 Hz) and 3.32 [3H, s, N(1)CH_3] (see Figure S1 of the Supporting Information). Spectral properties were in agreement with those reported previously.[23,24]

Uncatalyzed Deamination of 1-*N*-Methyl-5-fluorocytosine. In view of the known thermal instability of the product 5-fluorouridine,[25] the uncatalyzed deamination rate of 5-fluorocytidine was estimated using the model compound 1-*N*-methyl-5-fluorocytosine. Aqueous solutions of 1-*N*-methyl-5-fluorocytosine (0.01 M) in potassium phosphate buffer (0.1 M, pH 6.8) were sealed in quartz tubes under vacuum and incubated at elevated temperatures (90−140 °C) for varying periods of time. The contents were then diluted in D_2O and analyzed by ^{1}H NMR (Inova 500 MHz instrument, Varian, Palo Alto, CA) using pyrazine as an added integration standard (10^{-3} M). The results were compared to those of cytidine and 1-methylcytosine, which have been shown to be essentially identical.[26]

Effect of Fluorine on Hydrophobicity. To test whether the slow off rate or the lower $K_i^{observed}$ of FZeb (compared with that of Zeb) might be related to a simple difference in hydrophobicity, we sought to determine the effect of a single hydrogen-to-fluorine substitution on the ΔG of transfer of a related molecule from water to cyclohexane. The distribution coefficients of the tetrahydrofuryl derivative of 5-fluorouracil [1-(2-tetrahydrofuranyl)-5-fluorouracil] between water and cyclohexane were measured by a double-extraction procedure[27] and compared with that of the tetrahydrofuryl derivative of uracil.[28]

Synthesis of 5-Fluoro-1-methyl-2-oxopyrimidine (2). 7-Chloro-7-fluoro-2,5-dioxabicyclo[4.1.0]heptane was synthesized from 1,4-dioxene and dichlorofluoromethane according to the procedure of Molines et al.,[29] with a similar yield (~90%). The crude material was used to generate fluoromalonaldehyde bis(diethyl acetal) (**1**) by refluxing in ethanol containing sulfuric acid, as described by Molines et al.[29] Distillation (oil bath) afforded yields (~80%) equivalent to those reported previously.[29] **1** (200 mg, 0.8 mmol) was added to *N*-methylurea [60 mg (0.84 mmol), recrystallized from toluene prior to use] and cation exchange resin (2 g, AG 50W-X8, hydrogen form) in ethanol (1 mL) and concentrated HCl (1 mL) and heated (70 °C) while being stirred under argon. After ~2 h, the reaction mixture was filtered and the resin was washed with water until the filtrate no longer contained significant UV-absorbing material (predominantly a peak at 290 nm). The resin was then washed with ammonium hydroxide (0.25 M), and collected fractions were monitored for product by UV (λ_{max} = 336 nm)[16,30] in 1 M HCl. Fractions containing the product were pooled, and the ammonium hydroxide was removed under reduced pressure. The resultant white solid (18.3 mg, 20% yield) was triturated with cold ethanol to remove a trace impurity. Alternatively, the compound was purified by flash chromatography (silica) using ethyl acetate containing 5% methanol (v/v), with similar results. The product was also visualized on TLC plates by spraying with basic permanganate. ^{1}H and ^{19}F NMR values [25 mM potassium phosphate buffer (pH 7.0) containing 20% D_2O] for **2** were identical to the reported values under the same conditions.[16]

Synthesis of 5-Fluoro-1,3-dimethyl-2-oxopyrimidine (3). **1** (200 mg, 0.8 mmol) was added to *N*,*N*-dimethylurea [70 mg (0.8 mmol), recrystallized from toluene prior to use] in formic acid (90%, 2 mL) and heated (60−65 °C) while being stirred under argon. Product formation was monitored by UV

dx.doi.org/10.1021/bi300516u | *Biochemistry* 2012, 51, 6476−6486

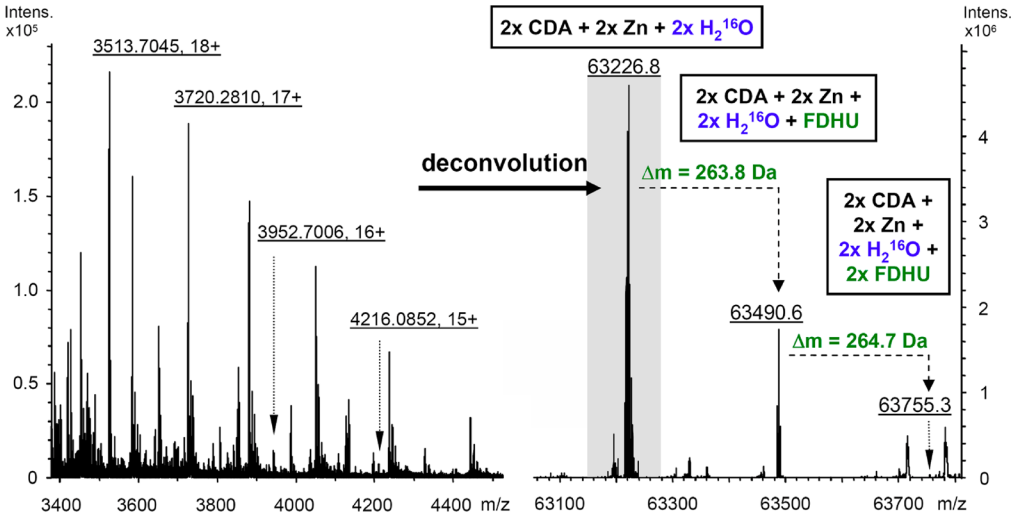

Figure 2. FTICR-MS analysis of CDA (nondenaturing conditions) in the presence of FZeb in $H_2{}^{16}O$. Following deconvolution of the multiply charged ion signals, the most significant peak corresponded to the mass of the enzyme dimer with two zinc atoms and two water molecules bound (shaded region). Additional peaks corresponding to the added mass of either one or two molecules of the hydrated inhibitor FDHU were also observed.

(337 nm)[16] in 1 M HCl, with concomitant loss of a peak at 256 nm. After 5 h, the formic acid was removed by rotary evaporation, yielding a yellow oil. The material was dissolved in a 1:1 ethyl acetate/hexane mixture (v/v), loaded onto a plug of silica, and eluted, first with 100 mL of the same solvent mixture and then with 100 mL of ethyl acetate. Rotary evaporation yielded a yellow oil, which was dissolved in a 1:1 ethanol/HCl mixture (1 M). A rotary evaporation of the solution yielded a yellowish solid, which was triturated with ethanol, yielding a fine white solid. The residual ethanol (colored yellow) was then decanted from the crystals that were subsequently washed with ethanol. The decanted ethanol solution was subjected to the same procedure, yielding additional white crystals. The white crystals (18.6 mg, 18% yield) migrated as a single spot on TLC. ^{1}H and ^{19}F NMR values [25 mM potassium phosphate buffer (pH 7.0) containing 20% D_2O] for **3** were identical to the reported values under the same conditions.[16]

Thermodynamics of FDHU Formation in Solution. Earlier, the equilibrium constant for FZeb hydration (FDHU formation) in free solution was estimated by comparing the equilibrium constants for the ionization of water (K_w), for protonation of 5-fluoro-1-methyl-2-oxopyrimidine (**2**, K_1), and for addition of hydroxide ion to the 5-fluoro-1,3-dimethyl-2-oxopyrimidinium ion (**3**, K'_2) according to the equation ($K_{hydration}$) shown in Figure 7.[4,16] In this work, the dependence of each equilibrium constant on temperature was determined to estimate the relative contributions of enthalpy and entropy to FZeb hydration in solution. The temperature dependence (15−65 °C) for the ionization constant of water was obtained from the tables of Mesmer and Herting.[31] The dependencies of K_1 and K'_2 on temperature were determined from the dissociation constant of the conjugate acids of **2** and **3**, respectively. Thus, a 0.05 M solution of **2** or **3** (0.5 M ionic strength, KCl) was titrated to its pK_a value at 25 °C, and the pH of the solution was then measured over a temperature range from 10 to 60 °C.

Isothermal Titration Calorimetry. ITC experiments were conducted with a Microcal (Northampton, MA) MSC calorimeter. Enzyme (CDA) solutions were dialyzed in potassium phosphate buffer (0.10 M, pH 7), and FZeb solutions were made using the dialysate. Immediately prior to use, both solutions were degassed and solutions of CDA (14.1 μM) were titrated with 25 injections (4 μL) of FZeb (287 μM) while being stirred (400 rpm). The amount of heat released following each injection was determined by integration of the calorimetric signal. The heat arising from binding was determined from the difference between the observed heat of interaction and the corresponding heat of dilution. Origin (version 5.0, MicroCal, Inc.)[32,33] was used for signal integration and data fitting (nonlinear regression, single-binding site model). Reported thermodynamic data represent an average of two independent titrations (25 °C).

RESULTS

FTICR-MS Analysis. The observed monoisotopic mass of the CDA monomer under denaturing conditions was 31520.855 Da (Figure S2A of the Supporting Information), which is within 0.25 ppm (0.008 Da) of the theoretically calculated monoisotopic mass. Under nondenaturing conditions, the spectrum shows isotopic resolution with 31539.0 Da as the most abundant isotopic mass of the monomer (Figure S2B of the Supporting Information), matching the expected average mass of the monomeric enzyme derived from the elemental composition (31538.96 Da). Notably, the same value for the most abundant isotopic mass (31539.02 Da) was observed previously for the monomer under denaturing conditions.[14] In the absence of Fzeb, CDA was found to be predominantly monomeric in the gas phase under nondenaturing conditions, but one additional major ion series corresponding to the CDA dimer with two zinc atoms bound (most abundant mass being 63191.8 Da) was also observed, as reported previously.[14] However, in the presence of FZeb, the dimeric form of the enzyme was greatly stabilized and the complexes identified previously[14] were observed (Figure 2). The most significant of those peaks (63226.8 Da, shaded region in Figure 2) corresponds to the mass of the dimeric enzyme, plus two zinc atoms and two water molecules (or two ammonium ions). The next most significant peak in this region exhibited an increase in mass of 263.8 Da, the mass of the covalent hydrate of FZeb (FDHU). There was also a small

dx.doi.org/10.1021/bi300516u | *Biochemistry* 2012, 51, 6476−6486

peak that corresponded to the additional mass of a second molecule of FDHU (CDA complex with two inhibitors bound).

To test whether water rather than ammonium ion was actually bound, the FTICR-MS experiment with CDA and FZeb was repeated in ^{18}O-labeled water. The results of those experiments, focusing on the most statistically significant peak (shaded region in Figure 2), are summarized in Figure 3. The top panel (Figure 3A) shows the various dimeric species observed in this mass region during MS analysis, labeled according to the convention used in Scheme 1. Mass peaks in the subsequent panels (Figure 3B–D) are annotated according to this scheme. Figure 3B shows the deconvoluted mass spectrum of CDA nebulized from $H_2{}^{16}O$ in the absence of an inhibitor. This single peak corresponds to the mass of the enzyme dimer with two zinc atoms bound. The next panel (Figure 3C) shows that the most abundant dimeric CDA species in the mass spectrum following preincubation with the inhibitor FZeb exhibited a mass increment of 35.0 Da, consistent with the binding of two molecules of $H_2{}^{16}O$. A small additional mass peak was also observed that might correspond to the loss of a single water molecule from this most abundant mass peak (decrease in mass of 17.9 Da). The final panel (Figure 3D) shows the results of the same experiment repeated in the presence of $H_2{}^{18}O$. Three peaks are clearly evident. The mass of the least abundant peak matches that of the native dimer (Figure 3B). The next two peaks are shifted by an additional mass of either 19.8 or 39.5 Da (most abundant), the mass of either one or two molecules of $H_2{}^{18}O$, respectively. That difference would not be expected if $NH_4{}^+$ were bound instead. The fact that all three species are observed furnishes additional evidence that water rather than $NH_4{}^+$ (or K^+, 39 Da) is the species bound (as outlined in Scheme 1, stages 3–5). Notably, no mass shifts related to the loss (or gain) of water molecules were observed in the experiments conducted with the enzyme in the absence of inhibitor (Figure 3B), or in the presence of Zeb (data not shown).

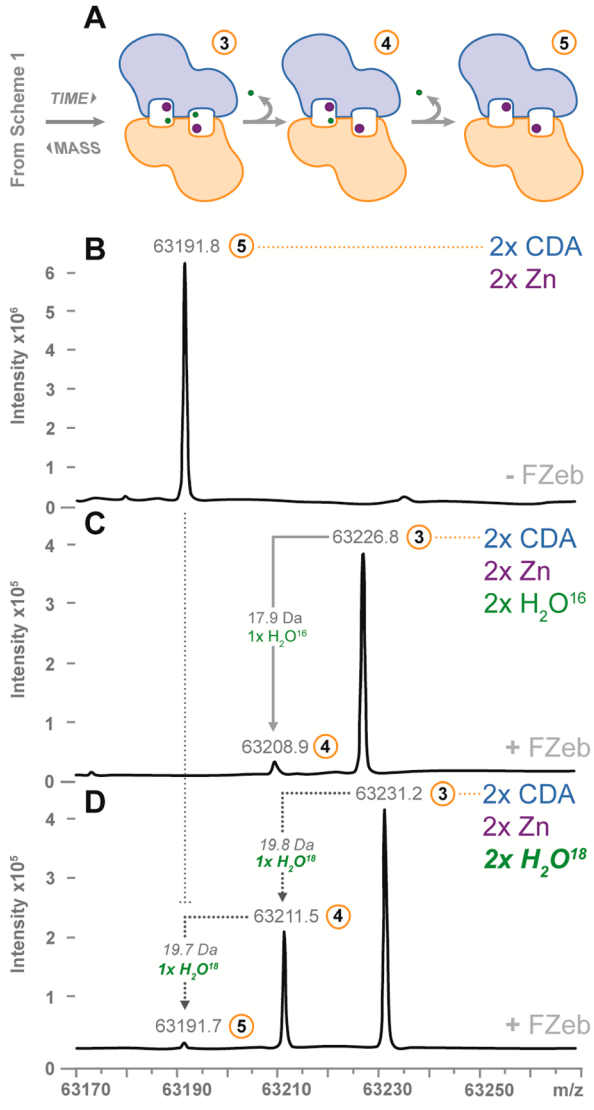

Figure 3. Deconvoluted FTICR mass spectra of dimeric CDA (nondenaturing conditions), with a scheme (A) illustrating the various species observed in this mass region (see Figure 2, shaded area). The components of the most significant peak in each spectrum (in daltons) are listed in each panel (right side). (B) CDA in $H_2{}^{16}O$ in the absence of an inhibitor. (C) CDA preincubated with the inhibitor FZeb in $H_2{}^{16}O$. Note the mass shifts of 17.1 or 35 Da from the apo form of the enzyme shown in panel B correspond to one or two $H_2{}^{16}O$ (or possibly one or two $NH_4{}^+$) molecules, respectively. (D) CDA preincubated with the inhibitor FZeb in $H_2{}^{18}O$. The least abundant peak corresponds to the apo form of CDA as seen in panel B (gray dotted lines). Note the additional mass shifts of either 19.8 or 39.5 Da, corresponding to one or two molecules of bound $H_2{}^{18}O$, respectively.

Pre-Steady State Kinetics for the Release of FZeb or Zeb. A plot of the time-dependent release of FZeb from CDA (Figure 4A) showed a clearly defined lag phase prior to steady state turnover (solid line, extrapolated from the final 200 s of the time course, gray). The difference (vertical distance) between the kinetic data trace and the extrapolated line (gray) is proportional to the concentration of the inhibited enzyme. A semilogarithmic plot of this distance versus time was used to determine the off rate constant (Figure 4B) of FZeb. The $t_{1/2}$ for release (vertical distance decreased by half) was ~60 s (k_{off} = 0.011 s^{-1}). The time of preincubation with the inhibitor (5–35 min) showed no effect on the observed off rate. Results with Zeb were identical to those of the uninhibited enzyme (data not shown).

Pre-Steady State Kinetics for the Binding of FZeb. Stopped-flow traces for the decrease in FZeb fluorescence with binding, in the presence of increasing concentrations of CDA are shown in Figure 5. The kinetic curves fit satisfactorily to a single exponential [R^2 = 0.99 (data not shown)], and the resultant apparent first-order rate constants (k_{obs}) obtained are plotted as a function of enzyme concentration in Figure 5 (inset). Fitting the data to eq 3 yields the following initial estimates for the binding rate constants: k_{on} = 3.7 × 10^5 M^{-1} s^{-1}, and k_{off} = 0.01 s^{-1}. Using these parameters as initial estimates, the full time course data were fit by simulation (KinTek Explorer)[20] to a single-step kinetic model for reversible inhibitor binding (eq 1), yielding the solid lines in Figure 5 and the following values: k_{on} = (4.1 ± 0.2) × 10^5 M^{-1} s^{-1}, and k_{off} = 0.016 ± 0.002 s^{-1}. Error limits were estimated using FitSpace[34] and reflect a 10% deviation from the minimal sum squared error of the best fit, which was well constrained. Taking an average of the off rate constant determined by competition assay (*vida supra*) with the value determined by this analysis, we determined a final value for k_{off} of 0.014 ± 0.003 s^{-1}. The dissociation constant, determined as the ratio of k_{off}/k_{on} [(3.4 ± 0.5) × 10^{-8} M], is within experimental error of the value reported previously, 3.5 × 10^{-8} M, for the $K_i^{observed}$ of

dx.doi.org/10.1021/bi300516u | *Biochemistry* 2012, 51, 6476–6486

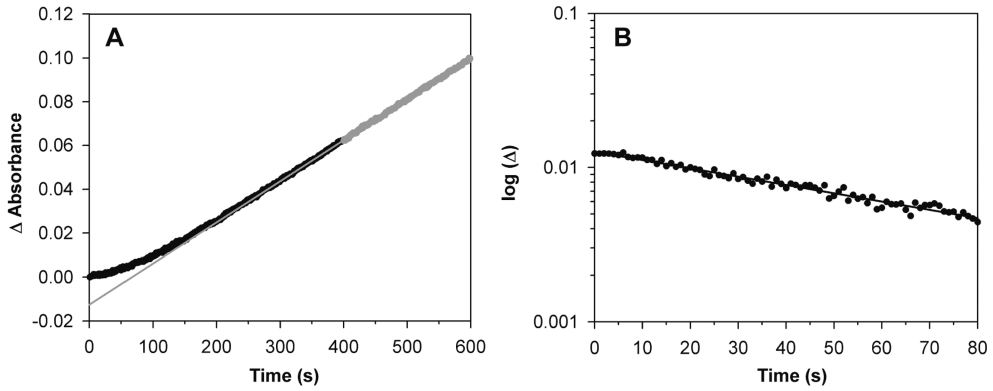

Figure 4. Competition assay (with excess cytidine) to determine the rate of release of CDA from Fzeb inhibition. (A) Time-dependent release from inhibition following preincubation (20 min) of CDA with Fzeb. (B) Semilog plot of the vertical distance between the extrapolated line (gray) and kinetic trace vs time. The $t_{1/2}$ for release from inhibition is calculated as the time for this distance to decrease by half (63 s). Accordingly, k_{off} was calculated to be 0.011 s^{-1} [$k_{off} = \ln(2)/t_{1/2}$].

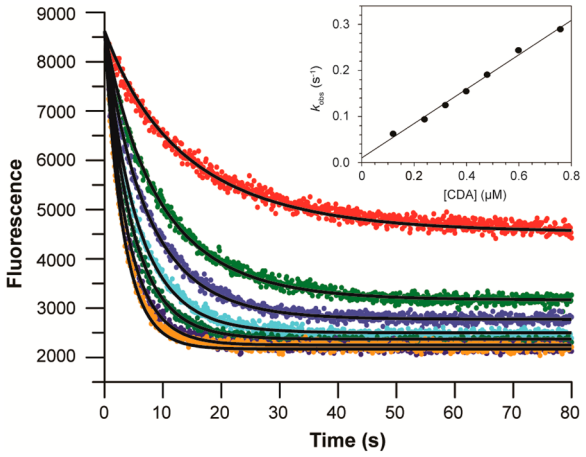

Figure 5. Stopped-flow fluorescence changes of FZeb (0.1 μM, after mixing) upon binding to CDA. Each trace represents an average of five experiments. The solid lines represent simulated fits to the data according to the model for reversible binding of an inhibitor to an enzyme in a single step (eq 1), with k_{on} and k_{off} rates of (4.1 ± 0.2) × 10^5 M^{-1} s^{-1} and 0.016 ± 0.002 s^{-1}, respectively. The inset corresponds to a plot of k_{obs} (single-exponential fit) vs enzyme concentration. The solid line corresponds to a linear fit to the data (R^2 = 0.99) and yielded initial estimates for k_{on} and k_{off} (where $k_{obs} = k_{on}[E] + k_{off}$).

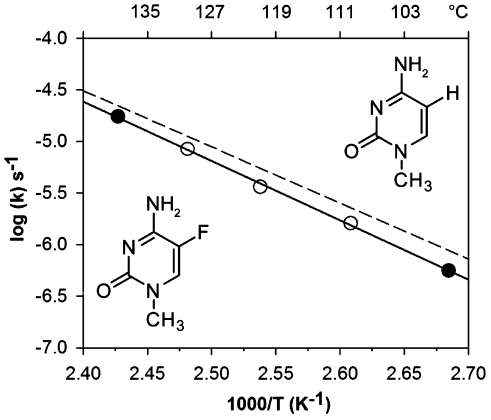

Figure 6. Arrhenius plot of the apparent first-order rate constants for the decomposition of 1-*N*-methyl-5-fluorocytosine at neutral pH. The k_{obs} values for the solid points (●) were determined by nonlinear regression analysis of time course data (see Figure S4A,B of the Supporting Information). The solid line is a linear fit to the data (R^2 = 0.99), and the dashed line represents the Arrhenius plot for 1-methylcytosine deamination, included for reference. Extrapolation (solid line) to 25 °C yields a nonenzymatic rate of deamination (k_{non}) of 7.5 × 10^{-11} s^{-1} ($t_{1/2}$ ~ 300 years).

FZeb.[17] The latter value will be used in the discussion that follows.

Steady State Kinetics of Deamination. Initial rates of the enzyme-catalyzed deamination of both 5-fluorocytidine and cytidine are plotted versus substrate concentration in panels A and B of Figure S3 of the Supporting Information. Both substrates followed Michaelis−Menten kinetics, and the fitted lines represent a nonlinear regression fit (R^2 = 0.99) to the equation $v = k_{cat}[S]/(K_M + [S])$, where v is the initial rate and [S] is the substrate concentration. The kinetic parameters observed for 5-fluorocytidine were as follows: k_{cat} = 240 ± 10 s^{-1}, and K_M = 80 ± 5 μM. Those for cytidine were as follows: k_{cat} = 320 ± 10 s^{-1}, and K_M = 60 ± 5 μM.

Uncatalyzed Deamination of 1-*N*-Methyl-5-fluorocytosine. Apparent first-order rate constants for the neutral deamination of 1-*N*-methyl-5-fluorocytosine are shown as a linear Arrhenius plot in Figure 6 (solid line). The Arrhenius plot for the deamination of 1-*N*-methylcytosine (k_{non} = 2 × 10^{-10} s^{-1} at 25 °C)[26] is also included for reference (Figure 6, dashed line). The data points at 100 and 140 °C reflect nonlinear regression fits of time course data to a single exponential (see Figure S4A,B of the Supporting Information). In both cases, fits were satisfactory (R^2 = 0.99) and indicate that the reaction is first-order. The observed free energy of activation ($\Delta G^{\ddagger}$) of the reaction was 31.2 kcal/mol, with a $\Delta H^{\ddagger}$ of 26 kcal/mol and a $T\Delta S^{\ddagger}$ of −5.2 kcal/mol. By extrapolation, the rate constant (k_{non}) for 1-*N*-methyl-5-fluorocytosine deamination at 25 °C is 7.5 × 10^{-11} s^{-1} ($t_{1/2}$ ~ 300 years). CDA therefore generates a rate enhancement (k_{cat}/k_{non}) of 3 × 10^{12} for the deamination of 5-fluorocytidine that is somewhat greater than the value for cytidine (1 × 10^{12}).[4]

Effect of Fluorine on Hydrophobicity. The tetrahydrofuryl derivative of 5-fluorouracil had a ΔG of transfer from water to cyclohexane of 4.8 ± 0.2 kcal/mol, which can be compared to the value of 5 ± 0.2 kcal/mol[28] for the tetrahydrofuryl derivative of uracil. It is therefore unlikely that the 10-fold lower $K_i^{observed}$ of FZeb compared to that of Zeb arises from a simple difference in the hydrophobicity of these molecules.

dx.doi.org/10.1021/bi300516u | *Biochemistry* 2012, 51, 6476−6486

Thermodynamics of FDHU Formation in Solution. The thermodynamic changes associated with FZeb hydration in free solution were estimated by measuring the temperature dependence for protonation of 5-fluoro-1-methyl-2-oxopyrimidine (K_1), for hydroxide addition to 5-fluoro-1,3-dimethyl-2-oxopyrimidinium (K'_2), and for the ionization of water (K_w), as shown in Figure 7. The temperature dependence of K_1 and K'_2

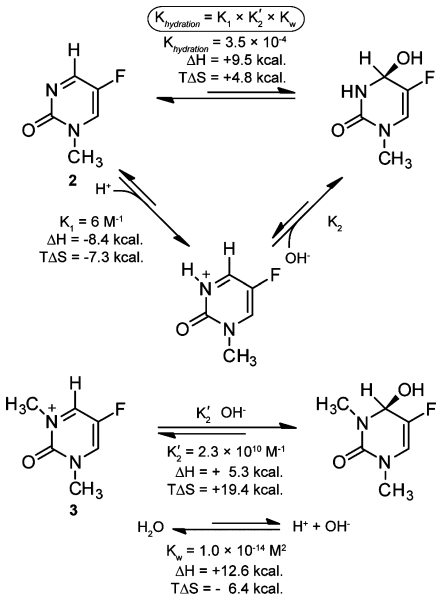

Figure 7. Thermodynamic changes associated with the equilibrium constant for hydration of 5-fluoro-1-methyl-2-oxopyrimidine (**2**), based on the thermodynamic changes accompanying the ionization of water to generate a proton and hydroxide anion (K_w),[31] addition of a proton to the C=N bond (K_1), and addition of a hydroxide anion to the protonated C=N bond (K_2). The parameters associated with K_2 were estimated by modeling, utilizing addition of a hydroxide anion to the quaternary amine formed by N-methylation (K'_2, **3**). Values for the equilibrium constants at 25 °C were obtained as described in ref 16.

yielded linear van't Hoff plots from 10 to 60 °C (Figure S5A,B of the Supporting Information), corresponding to ΔH values of −8.4 ± 0.2 and 5.3 ± 0.1 kcal/mol (25 °C), respectively.

Isothermal Titration Calorimetric Study of FZeb Binding by Cytidine Deaminase. Binding of FZeb was exothermic with a ΔH_{cal} of −13.6 ± 0.2 kcal/mol, after subtraction of the heat of dilution of the inhibitor, measured after binding saturation (Figure S6 of the Supporting Information). The K_d value determined at 25 °C from nonlinear fitting of the titration data (single-binding site model) was within 2-fold of the $K_i^{observed}$ value reported earlier for this complex (3.5×10^{-8} M).[17] Using the relationship $\Delta G = \Delta H - T\Delta S$, an entropy change of −3.5 ± 0.2 kcal/mol (25 °C) was estimated for the binding of FZeb.

DISCUSSION

When nebularized under nondenaturing conditions, CDA is predominantly monomeric in the vapor phase, and zinc is absent (this work and ref 14). The native dimer is also observed, retaining both zinc atoms but devoid of water molecules. In view of the high vacuum of the analysis chamber, and experimental evidence that implies that the formation of the zinc-bound hydroxyl (Figure 1) occurs after substrate binding,[6] the absence of water is not surprising. When CDA is

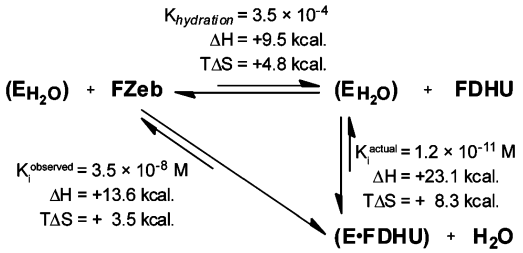

Figure 8. Thermodynamic cycle used to estimate the equilibrium constant (K_i^{actual}) for dissociation of the enzyme−FDHU complex along with the relative contributions of enthalpy and entropy. The value of $K_i^{observed}$ for FZeb was taken from ref 17.

nebularized after preincubation with FZeb, the relative abundance of the dimeric form increases ~10-fold but remains ~10-fold lower than that of the monomer. Under these conditions, new masses are observed (Figure 2) that correspond to the native dimer and an added mass of 35 Da, along with other mass peaks further shifted by the mass of either one or two molecules of the covalent hydrate of FZeb (FDHU). The experiments with ^{18}O-labeled water and FZeb presented here exhibited an added mass of 39.5 Da (vs 35 Da), indicating that this added mass corresponds to two additional water molecules ($H_2{}^{18}O$) rather than ammonium ions (Figure 3). In every experiment with FZeb, the most abundant dimeric form of CDA contained the additional mass of two water molecules.[35] Apparently, the covalently hydrated inhibitor molecules "leak" out over time, followed by the trapped water molecules, yielding the additional peaks observed (Scheme 1).

As noted in our original publication,[14] the entire complex remains intact in the vapor phase, at least for the 2−3 s required for analysis. Thus, the enzyme appears to retain a somewhat native-like conformation, at least in the region of the active site. FDHU binds across the dimeric interface of CDA, and <0.1% of the bound inhibitor is exposed to bulk solvent.[8] It seems likely that a water molecule is trapped in the product ammonium ion binding pocket behind the pyrimidine ring of the inhibitor [as observed when product is bound (see Figure 1A,B)], and that the presence of FDHU counteracts the tendency of the dimer to dissociate by acting as a kind of "noncovalent cross-link" across the dimer interface. The apparent stability of the enzyme−water complex may simply represent the steady state concentration of this species in the vapor phase.

A growing body of work[36−38] indicates that nebularization is an effective sampling method, furnishing a snapshot[37] of the situation in solution. Accordingly, the kinetic stability of the FZeb−CDA complex in solution was also investigated, with the results shown in Figures 4 and 5. In solution, the kinetic barrier to dissociation of FZeb from CDA is substantial (k_{off} = 0.014 s^{-1}), equivalent to a $t_{1/2}$ of ~1 min, which could be related to the stability of the complex in the vapor phase. In similar experiments that aimed to measure the dissociation of Zeb from CDA in solution, there was no evidence of slow release from inhibition: a lower limit for k_{off} can be estimated to be 0.14 s^{-1} ($t_{1/2}$ ~ 5 s) based on the dead time of the experiment. On the basis of this lower limit, an on rate exceeding the diffusion limit would be required to account for the observed inhibition constant of Zeb ($K_i^{observed} = 4.6 \times 10^{-7}$ M), implying that DHU must be generated by hydration at the active site (see also ref 17). This kinetic instability may help to explain

dx.doi.org/10.1021/bi300516u | *Biochemistry* 2012, 51, 6476−6486

Table 1. Comparison of Kinetic and Thermodynamic Parameters for Binding of Zeb and FZeb to CDA

	zebularine	5-fluorozebularine	result of fluorine addition
k_{on}	rapid	$4.1 \pm 0.2 \times 10^5$ $M^{-1}s^{-1}$	binding no longer rapid equilibrium process
k_{off}	> 0.14 s^{-1}	0.014 ± 0.003 s^{-1}	**slow release of fluorinated inhibitor ($t_{1/2}$ ~50 s)**
$K_i^{observed}$	2.9×10^{-7} M [a]	3.5×10^{-8} M [b]	~10-fold increase in affinity (apparent)
ΔH^{dissoc}	+10.0 kcal/mol [a]	+13.6 kcal/mol [c]	~3 kcal/mol increase in enthalpic barrier to release
$T\Delta S^{dissoc}$	+1.1 kcal/mol [a]	+3.5 kcal/mol	~2 kcal/mol reduction in entropic barrier to release
$K_{hydration}$	4.5×10^{-6} [a]	3.5×10^{-4}	~70-fold increase in favorability of hydration (K_{eq})
$\Delta H^{hydration}$	+11.1 kcal/mol [a]	+9.5 kcal/mol [d]	~2 kcal/mol reduction in enthalpic barrier to hydration
$T\Delta S^{hydration}$	+3.8 kcal/mol [a]	+4.8 kcal/mol [d]	~1 kcal/mol reduction in entropic barrier to hydration
K_{tx}	1×10^{-16} M [a]	2×10^{-17} M [e]	~5-fold increase in ideal transition state (hydrate) affinity
K_i^{actual}	1.3×10^{-12} M [a]	1.2×10^{-11} M [f]	**covalent hydrate (FDHU) is bound 10-fold less tightly**
ΔH^{dissoc}	+21.1 kcal/mol [a]	+23.1 kcal/mol [f]	~2 kcal/mol increase in enthalpic barrier to hydrate release
$T\Delta S^{dissoc}$	+4.9 kcal/mol [a]	+8.3 kcal/mol [f]	~3 kcal/mol reduction in entropic barrier to hydrate release [g]
$\Delta\Delta G^{K_{tx}\text{-}K_i}$	+5.6 kcal/mol [h]	+7.9 kcal/mol [h]	**energetic shortfall matches entropic cost of binding**

[a]Values taken from ref 4. [b]Value reported in ref 17; k_{off}/k_{on}. [c]Determined by ITC measurements with the inhibitor FZeb. [d]Estimated using **2** and **3** (see Figure 7 and the corresponding text). [e]$K_{tx} = k_{non}/(k_{cat}/K_m)$, with k_{non} estimated using the model compound *N*1-methyl-5-fluorocytosine (see the text). [f]See the thermodynamic cycle in Figure 8 and the corresponding text. [g]Note that the liberation of a trapped water molecule would be entropically favorable. [h]$\Delta\Delta G^{K_{tx}\text{-}K_i} = -RT \ln(K_{tx}/K_i^{actual})$.

why experiments with Zeb failed to generate the dimeric species observed by MS analysis with FZeb, despite the fact that the covalent hydrate of Zeb (DHU) is bound 10-fold more tightly than is FDHU.

It seems plausible that the stability of the FDHU complex in the vapor phase reflects kinetic rather than thermodynamic stability. The inhibitor 3,4,5,6-tetrahydrouridine (THU, structurally identical to DHU, but lacking the 5,6 double bond) exhibits a slow off rate ($t_{1/2} \sim 1$ min),[39] like that of FZeb, but is bound ($K_d \sim 10^{-7}$ M)[17] ~10^4-fold less tightly than FDHU. Preliminary MS experiments with CDA and THU yielded peaks that corresponded to the mass of (A) the native dimer with both zinc atoms and two water molecules and (B) the native dimer with both zinc atoms, two water molecules, and two molecules of THU (data not shown). That result is consistent with the view that the barrier to complex dissociation in the gas phase is predominantly kinetic in origin. Notably, the presence of a trapped water molecule in the presence of THU was previously postulated on the basis of thermodynamic evidence.[40] It is of interest that a recent paper,[41] using a different MS approach (quadrupole time of flight), reports findings consistent with the presence of noncovalently bound water molecules trapped in a different enzyme−inhibitor complex in the vapor phase.

The origin of the slow binding [$k_{on} = (4.1 \pm 0.2) \times 10^5$ M^{-1} s^{-1}] and release of FZeb, relative to that of Zeb, is not immediately apparent. The region of the active site surrounding the fluorine atom is predominantly hydrophobic, with three nearby aromatic residues (Phe-71, Tyr-126, and Phe-165′) and the ring "face" (with a partial negative charge) of Phe-165′ oriented toward the fluorine atom.[8] To test whether an increase in hydrophobicity might be responsible for the observed kinetic stability of the fluorine derivative, we measured the distribution coefficient from water to cyclohexane of the fluorinated product analogue, 1-(2-tetrahydrofuranyl)-5-fluorouracil. The free energy of transfer from water to cyclohexane (4.8 ± 0.2 kcal/mol) was found to be the same, within experimental error, as that observed earlier for 1-(2-tetrahydrofuranyl)uracil (5.0 ± 0.2 kcal/mol). An alternative possibility is that the kinetic barrier to FDHU release, but not DHU release, is linked to a slow conformational change of the protein when the fluorinated inhibitor is bound. Such a change was previously postulated to explain the slow release of THU.[39]

In view of the ~70-fold more favorable hydration of FZeb versus Zeb in solution [which is presumably responsible (at least in part) for the lower $K_i^{observed}$ of FZeb],[16,17] it seemed possible that the addition of a fluorine atom at C5 might affect the uncatalyzed and enzymatic deamination rates to differing extents, resulting in a difference in transition state affinities between the two reactions. The uncatalyzed deamination of 5,6-dihydrocytidine (lacking the double bond) was previously found to proceed 10^5-fold more rapidly than that of cytidine.[40] We therefore determined the relevant parameters for both the uncatalyzed deamination of the model compound 1-*N*-methyl-5-fluorocytosine (k_{non}) and the enzymatic deamination of 5-fluorocytidine (k_{cat} and K_M), and these were compared with the corresponding parameters for the natural substrate cytidine. Fluorine addition led to a ~4-fold reduction in the rate of nonenzymatic deamination ($k_{non} = 7.5 \times 10^{-11}$ s^{-1}) compared with that of cytidine ($k_{non} = 2.7 \times 10^{-10}$ s^{-1}).[42] We also observed a slight reduction (<2-fold) in the value of k_{cat}/K_M (3×10^6 M^{-1} s^{-1}) compared with that of cytidine (this work). The virtual dissociation constant of the enzyme−substrate complex in the transition state for 5-fluorocytidine deamination (K_{tx}) can therefore be estimated to be 2×10^{-17} M [$k_{non}/(k_{cat}/K_M)$], which differs by only ~5-fold from the K_{tx} value for cytidine deamination [10^{-16} M (Figure 1)].

Transition state analogue inhibitors, because of their limited geometric and electronic resemblance to the altered substrate in the transition state, fall short of capturing the ideal binding affinity. To more fully understand the functional basis of that difference in binding affinity, it was of interest to measure and compare the thermodynamic changes that accompany the equilibrium binding of these inhibitors with those of the actual transition state. Thermodynamic parameters associated with FDHU formation in solution were estimated using model compounds **2** and **3** (Figure 7). In conjunction with the experimentally determined thermodynamic parameters for FZeb binding (ITC), a thermodynamic cycle of equilibria can be assembled to estimate the equilibrium constant (K_i^{actual}) and the corresponding contributions of enthalpy and entropy to dissociation of the enzyme−FDHU complex (Figure 8).

dx.doi.org/10.1021/bi300516u | *Biochemistry* 2012, 51, 6476−6486

Table 1 summarizes the results of this thermodynamic analysis and shows the effects of fluorine on the kinetics and thermodynamics of inhibitor binding. Perhaps most striking is the increase in kinetic stability introduced by fluorine addition.

FDHU falls short of capturing the expected free energy of binding of an ideal transition state analogue by 7.9 kcal/mol, as indicated by the final entries in Table 1. That value closely matches the entropic cost ($T\Delta S$ = −8.3 kcal/mol) associated with FDHU binding (shaded entries in Table 1). This result is consistent with the entropic penalty observed previously for Zeb binding[4] and seems understandable in terms of a trapped water molecule at the active site.

CONCLUSION

This work confirms the entropically unfavorable trapping by FDHU of noncovalently bound water by CDA, previously inferred from thermodynamic evidence. This appears to represent the first identification by FTICR-MS of an enzyme-bound water molecule in an active site situated at a subunit interface. Remarkably, this water molecule remains bound long enough to allow detection at the high vacuum levels present in the mass spectrometer. In principle, an analogue that displaced this water molecule might be a far better inhibitor.

ASSOCIATED CONTENT

Supporting Information

Additional ^{1}H NMR and MS spectra, along with Michaelis−Menten plots, uncatalyzed kinetic time course data, van't Hoff plots, and ITC results. This material is available free of charge via the Internet at http://pubs.acs.org.

AUTHOR INFORMATION

Corresponding Author

*G.K.S.: phone, (512) 471-8860; e-mail, gkschroeder@mail.utexas.edu. R.W.: phone, (919) 966-1203; fax, (919) 966-2852; e-mail, water1@ad.unc.edu.

Present Address

[§]Division of Medicinal Chemistry, College of Pharmacy, University of Texas, Austin, TX 78712.

Author Contributions

G.K.S. and L.Z. contributed equally to this work.

Funding

This work was supported by National Institutes of Health Grant GM-18325.

Notes

The authors declare no competing financial interest.

ACKNOWLEDGMENTS

We thank Ashutosh Tripathy for his assistance with the fluorescence data acquisition at the Macromolecular Interactions Facility (University of North Carolina) and William H. Johnson for his help and guidance with the synthesis of **2** and **3**.

ABBREVIATIONS

Zeb, zebularine; CDA, cytidine deaminase; FZeb, 5-fluorozebularine; DHU, 3,4-dihydrouridine; FTICR, Fourier transform ion cyclotron resonance; MS, mass spectrometry; FDHU, 5-fluoro-3,4-dihydrouridine; TLC, thin layer chromatography; ITC, isothermal titration calorimetry; THU, 3,4,5,6-tetrahydrouridine.

REFERENCES

(1) Wolfenden, R. (1972) Analog approaches to the structure of the transition state in enzyme reactions. *Acc. Chem. Res. 5*, 10−18.

(2) Lienhard, G. E. (1973) Enzymatic catalysis and transition-state theory. *Science 180*, 149−154.

(3) Wolfenden, R., and Snider, M. J. (2001) The depth of chemical time and the power of enzymes as catalysts. *Acc. Chem. Res. 34*, 938−945.

(4) Snider, M. J., and Wolfenden, R. (2001) Site-bound water and the shortcomings of a less than perfect transition state analogue. *Biochemistry 40*, 11364−11371.

(5) Navaratnam, N., Fujino, T., Bayliss, J., Jarmuz, A., How, A., Richardson, N., Somasekaram, A., Bhattacharya, S., Carter, C., and Scott, J. (1998) *Escherichia coli* cytidine deaminase provides a molecular model for ApoB RNA editing and a mechanism for RNA substrate recognition. *J. Mol. Biol. 275*, 695−714.

(6) Snider, M. J., Reinhardt, L., Wolfenden, R., and Cleland, W. W. (2002) ^{15}N kinetic isotope effects on uncatalyzed and enzymatic deamination of cytidine. *Biochemistry 41*, 415−421.

(7) Xiang, S., Short, S. A., Wolfenden, R., and Carter, C. W., Jr. (1995) Transition-state selectivity for a single hydroxyl group during catalysis by cytidine deaminase. *Biochemistry 34*, 4516−4523.

(8) Betts, L., Xiang, S., Short, S. A., Wolfenden, R., and Carter, C. W., Jr. (1994) Cytidine deaminase. The 2.3 Å crystal structure of an enzyme:transition-state analog complex. *J. Mol. Biol. 235*, 635−656.

(9) Xiang, S., Short, S. A., Wolfenden, R., and Carter, C. W., Jr. (1997) The structure of the cytidine deaminase-product complex provides evidence for efficient proton transfer and ground-state destabilization. *Biochemistry 36*, 4768−4774.

(10) DeLano, W. L. (2002) *The PyMOL Molecular Graphics System*, DeLano Scientific, San Carlos, CA.

(11) Baker, N. A., Sept, D., Joseph, S., Holst, M. J., and McCammon, J. A. (2001) Electrostatics of nanosystems: Application to microtubules and the ribosome. *Proc. Natl. Acad. Sci. U.S.A. 98*, 10037−10041.

(12) Dolinsky, T. J., Nielsen, J. E., McCammon, J. A., and Baker, N. A. (2004) PDB2PQR: An automated pipeline for the setup of Poisson-Boltzmann electrostatics calculations. *Nucleic Acids Res. 32*, W665−W667.

(13) Dolinsky Todd, J., Czodrowski, P., Li, H., Nielsen Jens, E., Jensen Jan, H., Klebe, G., and Baker Nathan, A. (2007) PDB2PQR: Expanding and upgrading automated preparation of biomolecular structures for molecular simulations. *Nucleic Acids Res. 35*, W522−W525.

(14) Borchers, C. H., Marquez, V. E., Schroeder, G. K., Short, S. A., Snider, M. J., Speir, J. P., and Wolfenden, R. (2004) Fourier transform ion cyclotron resonance MS reveals the presence of a water molecule in an enzyme transition-state analogue complex. *Proc. Natl. Acad. Sci. U.S.A. 101*, 15341−15345.

(15) Cohen, R. M., and Wolfenden, R. (1971) Cytidine deaminase from *Escherichia coli*. Purification, properties, and inhibition by the potential transition state analog 3,4,5,6-tetrahydrouridine. *J. Biol. Chem. 246*, 7561−7565.

(16) Carlow, D. C., Short, S. A., and Wolfenden, R. (1996) Role of glutamate-104 in generating a transition state analog inhibitor at the active site of cytidine deaminase. *Biochemistry 35*, 948−954.

(17) Frick, L., Yang, C., Marquez, V. E., and Wolfenden, R. V. (1989) Binding of pyrimidin-2-one ribonucleoside by cytidine deaminase as the transition-state analog 3,4-dihydrouridine and contribution of the 4-hydroxyl group to its binding affinity. *Biochemistry 28*, 9423−9430.

(18) Smith, A. A., Carlow, D. C., Wolfenden, R., and Short, S. A. (1994) Mutations affecting transition-state stabilization by residues coordinating zinc at the active site of cytidine deaminase. *Biochemistry 33*, 6468−6474.

(19) Yang, C., Carlow, D., Wolfenden, R., and Short, S. A. (1992) Cloning and nucleotide sequence of the *Escherichia coli* cytidine deaminase (ccd) gene. *Biochemistry 31*, 4168−4174.

(20) Johnson, K. A., Simpson, Z. B., and Blom, T. (2009) Global Kinetic Explorer: A new computer program for dynamic simulation and fitting of kinetic data. *Anal. Biochem. 387*, 20−29.
(21) Alderfer, J. L., Loomis, R. E., Sharma, M., and Hazel, G. (1985) Halogenated nucleic acids: Base properties and conformation of fluorinated derivatives. *Prog. Clin. Biol. Res. 172*, 249−261.
(22) Yamauchi, K., Tanabe, T., and Kinoshita, M. (1976) Methylation of nucleic acid-bases with trimethyl phosphate. *J. Org. Chem. 41*, 3691−3696.
(23) Durr, G. J. (1965) Some 5-fluoropyrimidines. *J. Med. Chem. 8*, 253−254.
(24) Atkins, P. J., and Hall, C. D. (1983) Stereochemistry of the formation of 4-alkoxyimino-5,6-dihydro-6-alkoxyaminopyrimidin-2(1H)-ones from cytosines and hydroxylamines. *J. Chem. Soc., Perkin Trans. 2,*, 155−160.
(25) Dorta, M. J., Munguia, O., Farina, J. B., Martin, V. S., and Llabres, M. (1997) Stability indicating high performance liquid chromatography methods for 5-fluorouridine in aqueous solution. *Arzneim. Forsch.,*, 1388−1392.
(26) Carlow, D., and Wolfenden, R. (1998) Substrate connectivity effects in the transition state for cytidine deaminase. *Biochemistry 37*, 11873−11878.
(27) Bone, R., Cullis, P., and Wolfenden, R. (1983) Solvent effects on equilibria of addition of nucleophiles to acetaldehyde and the hydrophilic character of diols. *J. Am. Chem. Soc. 105*, 1339−1343.
(28) Shih, P., Pedersen, L. G., Gibbs, P. R., and Wolfenden, R. (1998) Hydrophobicities of the nucleic acid bases: Distribution coefficients from water to cyclohexane. *J. Mol. Biol. 280*, 421−430.
(29) Molines, H., and Wakselman, C. (1989) Fluoromalonaldehyde bis(dialkyl acetals): Synthesis by carbene condensation and transformation to dialkyl fluoromalonates and fluorinated heterocyclic compounds. *J. Org. Chem. 54*, 5618−5620.
(30) Cech, D., Beerbaum, H., and Holy, A. (1977) Nucleic acid components and their analogs. CXCI. 5-Fluoro-2-pyrimidinone and its N1-substituted derivatives. *Collect. Czech. Chem. Commun. 42*, 2694−2700.
(31) Mesmer, R. E., and Herting, D. L. (1978) Thermodynamics of ionization of D_2O and $D_2PO_4^-$. *J. Solution Chem. 7*, 901−913.
(32) Indyk, L., and Fisher, H. F. (1998) Theoretical aspects of isothermal titration calorimetry. *Methods Enzymol. 295*, 350−364.
(33) Wiseman, T., Williston, S., Brandts, J. F., and Lin, L. N. (1989) Rapid measurement of binding constants and heats of binding using a new titration calorimeter. *Anal. Biochem. 179*, 131−137.
(34) Johnson, K. A., Simpson, Z. B., and Blom, T. (2009) FitSpace Explorer: An algorithm to evaluate multidimensional parameter space in fitting kinetic data. *Anal. Biochem. 387*, 30−41.
(35) Another mass peak corresponding to the additional mass of one FDHU molecule, albeit weak, was also observed in the $H_2{}^{18}O$ experiment (data not shown).
(36) Gao, J., Wu, Q., Carbeck, J., Lei, Q. P., Smith, R. D., and Whitesides, G. M. (1999) Probing the energetics of dissociation of carbonic anhydrase-ligand complexes in the gas phase. *Biophys. J. 76*, 3253−3260.
(37) Li, Z., Sau, A. K., Shen, S., Whitehouse, C., Baasov, T., and Anderson, K. S. (2003) A snapshot of enzyme catalysis using electrospray ionization mass spectrometry. *J. Am. Chem. Soc. 125*, 9938−9939.
(38) Yu, Y., Kirkup, C. E., Pi, N., and Leary, J. A. (2004) Characterization of noncovalent protein-ligand complexes and associated enzyme intermediates of GlcNAc-6-O-sulfotransferase by electrospray ionization FT-ICR mass spectrometry. *J. Am. Soc. Mass Spectrom. 15*, 1400−1407.
(39) Ashley, G. W., and Bartlett, P. A. (1984) Inhibition of *Escherichia coli* cytidine deaminase by a phosphapyrimidine nucleoside. *J. Biol. Chem. 259*, 13621−13627.
(40) Snider, M. J., Lazarevic, D., and Wolfenden, R. (2002) Catalysis by entropic effects: The action of cytidine deaminase on 5,6-dihydrocytidine. *Biochemistry 41*, 3925−3930.
(41) Wang, S., Lim, J., Thomas, K., Yan, F., Angeletti, R. H., and Schramm, V. L. (2012) A complex of methylthioadenosine/S-adenosylhomocysteine nucleosidase, transition state analogue, and nucleophilic water identified by mass spectrometry. *J. Am. Chem. Soc. 134*, 1468−1470.
(42) Snider, M. J., Gaunitz, S., Ridgway, C., Short, S. A., and Wolfenden, R. (2000) Temperature effects on the catalytic efficiency, rate enhancement, and transition state affinity of cytidine deaminase, and the thermodynamic consequences for catalysis of removing a substrate "anchor". *Biochemistry 39*, 9746−9753.